CHARACTERIZING FALSE POSITIVES IN CRISM VNIR FROST DETECTIONS P. Rupireddy[1], G. Doran[2], C. E. Viviano[3], S. Diniega[2], K. L. Wagstaff[2], S. F. A. Cartwright[3], K. Hancock[3], F. P. Seelos[3], K. D. Seelos[3], J. M. Widmer[4]. [1]University of Chicago (rupir001@uchicago.edu), [2]Jet Propulsion Laboratory, California Institute of Technology, [3]Johns Hopkins University Applied Physics Laboratory, [4]University of California, Los Angeles.

Introduction: The martian frost cycle is a key driver of both climate and geomorphological features on the surface of Mars. To better understand the martian frost cycle, we are interested in building global maps of frost across the Mars year using automated detection within visible, thermal, and other multispectral and hyperspectral observations. The CRISM (Compact Reconnaissance Imaging Spectrometer for Mars) instrument, which collects data in infrared (IR, 1.0–3.9 μm) and visible/near infrared (VNIR, 0.4–1.0 μm) wavelengths remotely from orbit, can be used for automated detection and importantly, enables the differentiation of frost types (CO_2 and H_2O). However, VNIR wavelengths, analyzed with the new "ICV" (from "ices in VNIR") spectral parameterization [1], typically produce less robust detections of frost compared with ICE (from "ices"), which uses both VNIR- and IR-derived parameters [2]. Our analysis characterizes some spectral properties that can lead to false positive frost detections using ICV. These results inform methods for excluding problematic observations when ICV is used for automated frost detection for global mapping.

Background: There are several science and engineering motivations for understanding the martian frost cycle. Frost deposition and sublimation drive large changes in pressure throughout the seasonal cycle, with significant effects on the martian climate [3]. Second, the frost cycle is hypothesized to be a driver of geomorphological feature formation and evolution on the martian surface, including frost-driven avalanches contributing to gully formation, and sublimation-driven jets that lead to araneiforms [4]. Frost can also impact surface operations, such as when it accumulated on *Phoenix* solar panels.

Prior work on martian frost mapping has utilized both visible High Resolution Imaging Experiment (HiRISE) and thermal Mars Climate Sounder (MCS) data for detection [5]. This work focuses on characterizing frost detection using observations made by the CRISM instrument, which unlike HiRISE and MCS, can differentiate between H_2O and CO_2 frost using diagnostic absorptions in the IR range. However, CRISM IR data acquisition was suspended in 2018 with the retirement of the cryosystem. This motivates the use of VNIR-only methods like ICV to cover the post-2018 observing period. For evaluation purposes, we use Map-Projected Targeted Reduced Data Records (MTRDRs) acquired in Hyperspectral Mode that include both VNIR and IR wavelengths.

In order to summarize a spectrum, scientists use spectral parameters, which are functions of the signal level at a selected set of wavelengths. For our purposes, the most important of these parameterizations is relative band depth, a measure of the strength of a spectral absorption feature relative to the continuum level. While ICE is a spectral parameterization that has been used to robustly detect frost using IR observations, ICV is intended to enable frost detection in VNIR-only observations. Given that the causes of false negative detections are relatively well-known (e.g., icy soil, transparent CO_2), the scope of the project is to focus on false positives. This, in turn, will allow us to better deploy the ICV map for automating frost detection.

Approach: Because we are interested in characterizing false positive detections using ICV, we focus on observations in the northern mid-latitude region during seasons when MCS-derived surface temperatures are well above the frost point. Therefore, all ICV-based frost detections are likely to be false positives.

Our evaluation dataset consists of 708 summertime MTRDR observations from the Planetary Data System (PDS). Following the recommended methodology for applying the ICV parameter map, we use pixels with a red-blue ratio (RBR) exceeding a value of 3 as an indication of surface frost [1]. The red-blue ratio is computed by dividing smoothed reflectance at 770 nm by that at 440 nm. Application of the RBR mask revealed 113 observations with at least one false positive pixel.

Each observation containing a positive pixel is processed by two pipelines to generate diagnostic plots for visual inspection and to extract quantitative information. The plotting pipeline creates visualizations for each observation containing a representation of the CRISM VNIR spectrum along with several parameter maps: ICV, ICE, and BDI1000VIS (indicative of mafic composition and a known confounder of ICV). The quantitative pipeline clusters pixels from observations containing false frost detections to determine whether they share common spectral characteristics. The features extracted for each pixel include the band depths at 800 and 530 nm (BD800 and BD530_2, two parameters of the ICV map), and the BDI1000VIS and RPEAK1 parameters, which initial analyses suggested would help to identify terrains likely to produce false positives.

To perform a clustering analysis, we use the mini-batch k-means algorithm, which is an adaptation of the standard k-means algorithm that performs iterative updates using subsets of the full dataset [6]. Because we want to analyze pixels across a representative set of terrains, and some observations contained many more false positives than others, at most 10 false positive pixels are

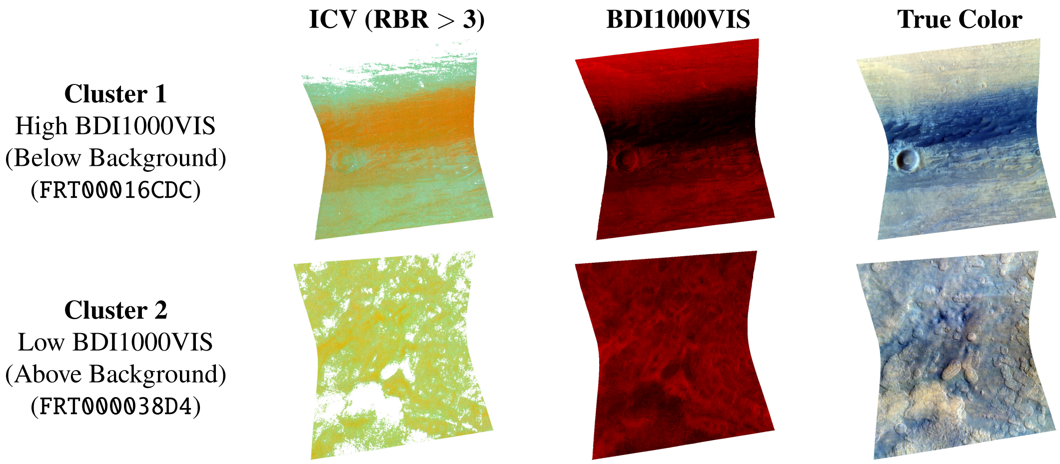

Figure 1: Examples of the two primary clusters in the dataset with high (top) and low (bottom) values of BDI1000VIS (middle) corresponding to the ICV false frost detections, colored pixels covering most of the scene (left). BDI1000VIS values are normalized, so they appear darker in Cluster 1 due to having values below that of surrounding pixels even though absolute values are above those in Cluster 2. Pixels in these clusters have Low BD530_2 values and tend to correspond to darker material in the visible image (right). Examples of Clusters 3 and 4 with High BD530_2 values are omitted since they typically consist of single pixels.

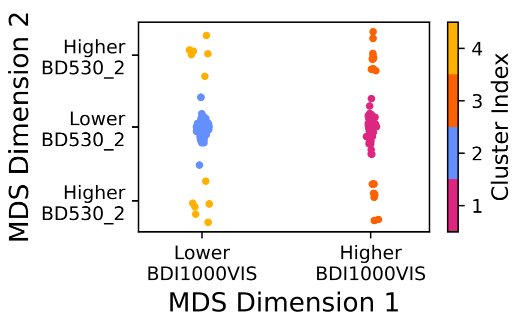

Figure 2: Clustering results projected into two-dimensions using multi-dimensional scaling (MDS). The two axes in this space primarily correspond to differences in BDI1000VIS and BD530_2 values across pixels.

sampled from each image. A value of $k = 4$ was determined empirically by increasing the value until further increases no longer split the samples into meaningful categories. The multi-dimensional scaling (MDS) algorithm is used map the multi-dimensional clustered data into a 2-dimensional space for visualization.

Results: We observe four distinct clusters in the data resulting from the combinations of two main factors: the level (High/Low) of BDI1000VIS as well as the level (High/Low) of the BD530_2 parameter. When these are cross-referenced with the visual plots, high values of BD530_2 are seen to correspond with single pixels corrupted by noise. Figure 1 shows representative examples of the clusters with low BD530_2 values, comprising the majority of false positive pixels. A plot of all clustered points projected using MDS is shown in Figure 2.

Analysis of the spectra within each cluster do not reveal any obvious data quality issues for Clusters 1 and 2, although the RPEAK1 parameters for Clusters 1 and 3 are null, and some spectra in Cluster 2 are deeply sloped between 775 and 975 nm. While further analysis is required, hypotheses to explain these clusters include the presence of mafic material, glasses, or aerosols.

Conclusions: In summary, after clustering false positive pixels attached to geophysical markers from over 100 summertime CRISM MTRDRs, we identified two underlying causes of systematic false positive pixels apart from noisy observations. The signatures of these false positives provide a strategy to mask out terrain when deploying ICV for frost detection during winter months.

In future work, we plan to include southern hemisphere observations in our analysis of false positives. We would also like to compare the frost detection efficacy of ICV to that of ICE. This requires determining a set of criteria for producing a binary frost mask from ICE to which ICV would be compared during the winter season. Once the performance of ICV has been characterized, we will better understand the possibilities and limitations of deploying it for automated frost detection and mapping.

Acknowledgments: We thank Steven Lu, Umaa Rebbapragada, and Mark Wronkiewicz, who contributed valuable feedback and guidance to this abstract. Part of this research was carried out at the Jet Propulsion Laboratory, California Institute of Technology, under a contract with the National Aeronautics and Space Administration (80NM0018D0004).

References: [1] Viviano *et al.* (2022) 53^{rd} *LPSC.* [2] Viviano *et al.* (2014) *JGR Planets.* [3] Diniega *et al.* (2020) *Planet. & Space Sci.* [4] Diniega *et al.* (2021) *Geomorph.* [5] Diniega *et al.* (2023) 54^{th} *LPSC.* [6] Sculley (2010) 19^{th} *WWW.*